PHOTOELECTROCHEMICAL STUDY OF PASSIVE LAYERS ON COPPER ELECTRODES IN SOME ALKALINE MEDIA ①

A. Kamkin[a, 1], Zhou Guoding[a], Xu Qunjie[b] and B. H.[c] Loo
[a] *Electrochemical Research Group, Shanghai Institute of Electric Power, Shanghai 200090, P. R. China*
[b] *Corrosion Prevention Center, East China University of Science and Technology, Shanghai 200237, P. R. China*
[c] *Department of Chemistry, University of Alabama, Huntsville, AL 35899, USA*
[a, 1] *Present address: Department of Chemistry, Moscow State University, Moscow, Russia*

ABSTRACT The electrochemical behavior of Cu electrodes in alkaline solutions with and without argon gas purging was studied by cyclic voltammetry and the photocurrent response method. In Na_2SO_4 solution (pH 9.1), the electrode shows a p-type photoresponse initially, which changes to an n-type when pitting corrosion occurs, at potentials more positive than the critical breakdown potential. The cathodic photocurrent is much larger in stronger alkaline solutions, e.g., 0.1 mol/L KOH solution, reflecting a more porous structure of Cu_2O layer on the electrode surface in strong alkaline solutions. Additionally, the cathodic current is larger in deaerated solutions than that in non-deaerated solutions. While the initiation of CuO formation on the electrode may not be obvious on the current-voltage curve, it can be obtained from the photocurrent-voltage curve where it corresponds to the onset of the decrease in the photocurrent on the positive potential scan.

Key words copper electrode alkaline solutions passive layer photocurrent response cyclic voltammetry

1 INTRODUCTION

The passive layer on the Cu electrode surface has been studied by the photoelectrochemical techniques[1-15]. In general, the passive layer is a simple Cu_2O layer or a duplex structure of the oxides, consisting of an inner Cu_2O layer and an outer $CuO/Cu(OH)_2$ layer. The inner layer thickness is in the range of 1~1.5 nm, while the outer layer grows with potential and time[16]. The Cu_2O layer on the Cu electrode in alkaline solution has a p-type semiconducting property with a bandgap of 3.1 eV for a direct transition, which gives rise to a cathodic photocurrent[6, 10-12]. It has been shown that the magnitude of the cathodic photocurrent can be correlated with the thickness of the Cu_2O film on the Cu electrode in alkaline solution[12, 17]. A photocurrent cannot be observed, however, from CuO on the Cu electrode because of its low resistivity and high recombination rate[12, 14].

The photoelectrochemical behavior of the Cu electrode depends on both the pH as well as the composition of the solution[1]. For examples, at lower pH, the n-type photoresponse appears, and the presence of Cu(II) species favors the n-type photoresponse[1, 15]; the p-type photoresponse is observed from Cu electrode in alkaline solutions in the absence of chloride ions. In the presence of chloride ions, however, the elec-

① Project 29070163 supported by the National Natural Science Foundation of China and Project 96QF32 supported by the Youth Science Foundation of Shanghai Higher Education Received Nov. 21, 1997; accepted Feb. 16, 1998

trode shows an n-type photoresponse, which is ascribed to the doping of the surface Cu_2O film by the Cl^- ions[7, 10, 12]. An n-type photoresponse is observed in solutions with 10^{-5}% or higher BTA concentration, and the magnitude of the anodic photocurrent increases with the BTA concentration[12]. Therefore, the photoelectrochemical behavior of the Cu electrode is closely associated with the nature of the surface oxides layer. In this work, we use cyclic voltammetry and the photoresponse method to study further the photoelectrochemical behavior of Cu electrode in deaerated and non-deaerated alkaline solutions, and examine the characteristics of the surface oxides layer at different pH and anodic switching potentials.

2 EXPERIMENTAL

A three-electrode cell with a flat optical glass was used. The reference electrode was a saturated calomel electrode (SCE) whereas the counter electrode was a Pt electrode. The working electrodes were prepared from 99.9% copper plates of 0.50 cm^2 area embedded in epoxy resin. The electrodes were polished with different grades of emery papers, and then washed, degreased with alcohol, and finally rinsed with deionized water. They were cathodically treated in a working electrolyte for 10 min prior to measurements. The electrolytes used were a borax buffer solution (0.075 mol/L $Na_2B_4O_7$ + 0.15 mol/L H_3BO_3, pH 8.5), 0.075 mol/L $Na_2B_4O_7$ (pH 9.2), 0.10 mol/L KOH and 0.05 mol/L Na_2SO_4 (pH 9.1), respectively.

The irradiation wavelength of a 1000 W Xe lamp was selected by using a WDG-1A monochromator (Siping Optical Instruments), with the spectral bandwidth smaller than 30 nm. A ND-4 chopper (Nanjing University) was used to modulate the light intensity, whereas a PARC M 5208EC lock-in analyzer was used to detect the signals. For spectral measurements, the light intensity was measured by a calibrated silicon photodiode, and the light flux never exceeded 2.0×10^{-2} W/cm^2. The photocurrent measurements were conducted at a light modulation frequency of 38 Hz and a wavelength of 420 nm. The potential control was provided by a PARC M273 potentiostat. The potentiodynamic scan rate was 2 mV/s. All potentials were referenced with respect to SCE.

3 RESULTS AND DISCUSSION

Fig. 1(a) shows the current density-voltage ($J-\varphi$) characteristics observed on a Cu electrode in an argon-gas-purged borax buffer solution (pH 8.5). Curves 1, 2 and 3 are the $J-\varphi$ plots with the anodic switching potentials φ_s of − 0.06, 0.30 and 0.80 V, respectively. The anodic peaks A_1 and A_2 correspond to the forma-

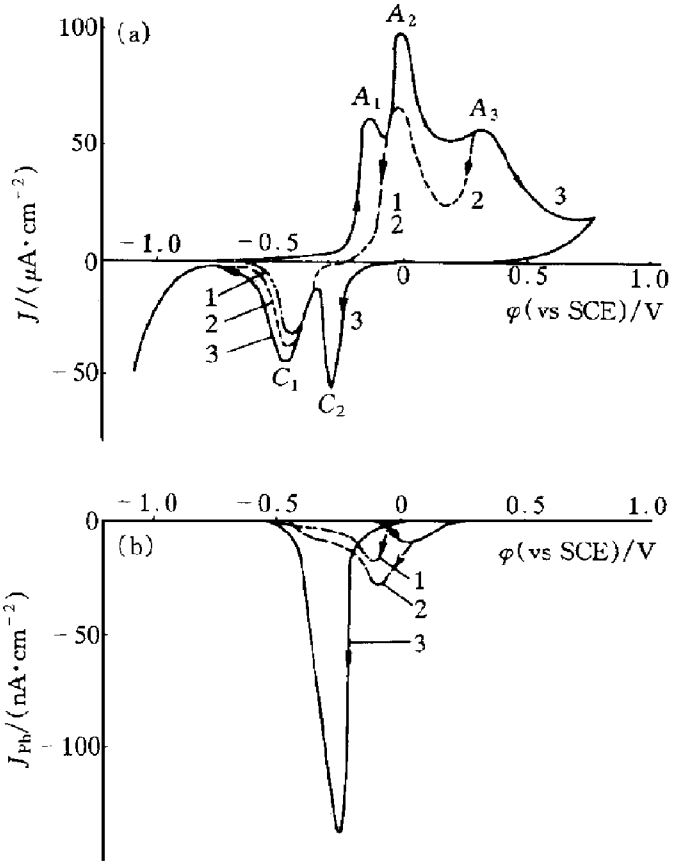

Fig. 1 (a) $J-\varphi$ curve and (b) $J_{ph}-\varphi$ curve for a Cu electrode in an argon-gas-purged borax buffer solution (pH 8.5) at different anodic switching potentials φ_s

(Scan rate 2 mV·s^{-1}, modulation frequency 38 Hz, irradiation wavelength 420 nm)
1 — − 0.06 V; 2 — 0.30 V; 3 — 0.80 V

tion of Cu (Ⅰ) from Cu(0), whereas the cathodic peak C_1 corresponds to the reduction of Cu(Ⅰ) to Cu(0)[12]. The peak A_3 is due to the anodic oxidation of Cu(Ⅰ) to Cu(Ⅱ), and the peak C_2 is due to the reduction of Cu(Ⅱ) to Cu (Ⅰ). Only one cathodic current peak C_1 is observed on the reverse negative scan when the φ_s is set at − 0.06 V.

Fig. 1(b) shows the corresponding photocurrent density vs voltage ($J_{ph}-\varphi$) curve. The photocurrents observed are of the p-type. On the positive potential scan, curves 2 and 3 overlap with each other at potentials cathodic to 0.25 V, and curve 1 also overlaps with curves 2 and 3 at potentials cathodic to − 0.06 V. The J_{ph} increases from − 0.14 V to 0.06 V, which may be correlated with the amount of Cu_2O formed on the Cu electrode. In the potential region from 0.06 V to 0.24 V, J_{ph} decreases with increasing potential, and finally disappears when the potential becomes more positive than 0.24 V. The decrease in the photocurrent is attributed to the oxidation of Cu_2O to CuO[12]. Although CuO is a narrow bandgap semiconductor with E_g = 0.60 eV[6], photocurrent has not been observed from CuO on the Cu electrode because of its low resistivity and high recombination rate[14]. Therefore, the initial decrease in the photocurrent may be taken as the onset of the formation of CuO on the electrode surface.

On the negative potential scan, J_{ph} gradually increases as CuO is reduced to Cu_2O, and then decreases as Cu_2O is gradually reduced to Cu. At potentials more negative than − 0.58 V, J_{ph} is close to zero as the reduction of Cu_2O is almost complete; the electrode surface is nearly reduced to the metallic state. Since the anodic switching potential in curve 3 is the most positive one (0.8 V), it is obvious that the largest amount of CuO is formed on the positive scan. Hence, on the reverse negative potential scan, the largest amount of Cu_2O is also produced, which results in the largest photocurrent among these three curves.

The $J-\varphi$ and $J_{ph}-\varphi$ plots for the Cu electrode in non-deaerated borax buffer solution (pH 8.5) are shown in Fig. 2(a) and 2(b), respectively. Curves 1, 2, 3 refer to the $J-\varphi$ plots with the anodic switching potentials φ_s of − 0.06, 0.30, and 0.80 V, respectively, as in the previous case. Comparing Fig. 1(a) and Fig. 2(a), it can be seen that there is a larger cathodic current from − 1.0 V to − 0.20 V on the positive potential scan when the solution is not purged of oxygen. The larger current is due to the reduction of the dissolved oxygen in the solution. Comparing Fig. 1(b) and Fig. 2(b), it can be seen that the magnitude of the photocurrent in Fig. 2(b) is less than half of that in Fig. 1 (b). This demonstrates that the amount of Cu_2O formed on the electrode surface in the presence of dissolved oxygen is much less than that in the absence of dissolved oxygen. This may be because the anodic dissolution of copper

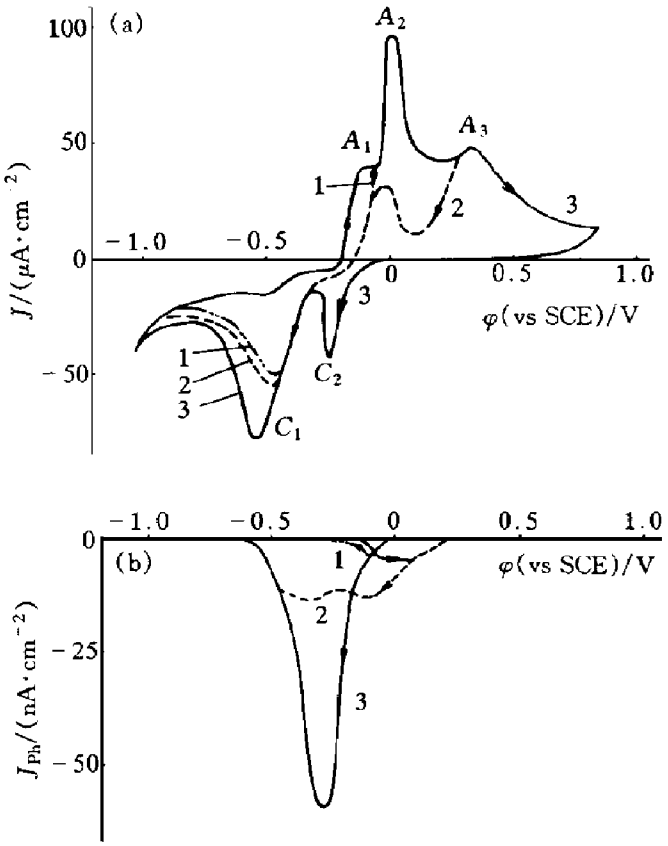

Fig. 2 (a) $J-\varphi$ curve and (b) $J_{ph}-\varphi$ curve for a Cu electrode in an non-deaerated borax buffer solution (pH 8.5) at different anodic switching potentials φ_s

(Scan rate 2 mV·s^{-1}, modulation frequence 38 Hz, irradiation wavelength 420 nm)
1 — − 0.06 V; 2 — 0.30 V; 3 — 0.80 V

is enhanced in the presence of dissolved oxygen, resulting in a smaller amount of Cu_2O on the electrode surface.

Fig. 3(a) and Fig. 3(b) show the $J-\varphi$ and $J_{ph}-\varphi$ plots for the Cu electrode in argon-gas-purged 0.075 mol/L $Na_2B_4O_7$ solution (pH 9.2), respectively. Curves 1 and 2 correspond to φ_s= 0.1 V and 0.8 V, respectively. In 0.075 mol/L $Na_2B_4O_7$ solution, both the current and photocurrent are smaller than the corresponding ones in the borax buffer solution (pH 8.5).

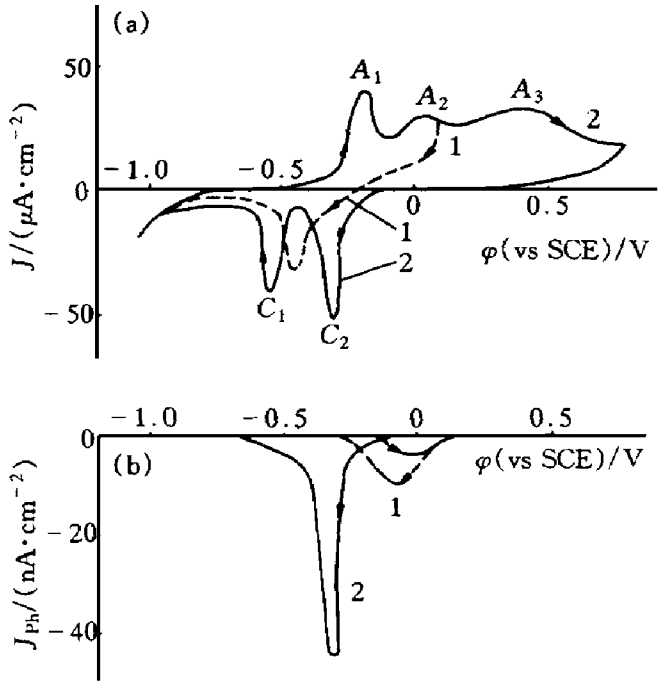

Fig. 3 (a) $J-\varphi$ curve and (b) $J_{ph}-\varphi$ curve for a Cu electrode in an argon-gas-purged 0.075 mol/L $Na_2B_4O_7$ solution (pH 9.2) at different anodic switching potentials φ_s

(Scan rate 2 mV·s^{-1}, modulation frequency 38 Hz, irradiation wavelength 420 nm)
1 —0.1 V; 2 —0.80 V

Fig. 4(a) and Fig. 4(b) show the $J-\varphi$ and $J_{ph}-\varphi$ plots for the Cu electrode in argon-gas-purged 0.1 mol/L KOH solution, respectively. Curves 1, 2, 3 and 4 correspond to φ_s= −0.24 V, −0.13 V, 0.20 V and 0.63 V, respectively. Compared with Fig. 1(a), the peak A_3 is greatly increased. In addition to the CuO and $Cu(OH)_2$ on the electrode surface, CuO_2^{2-} may be formed according to the following equations[18]:

$$Cu + 4OH^- \longrightarrow CuO_2^{2-} + 2H_2O + 2e$$

$$Cu_2O + 6OH^- \longrightarrow 2CuO_2^{2-} + 3H_2O + 2e$$

On the reverse scan, peak C_2 is much smaller than the peak A_3, indicating that a large amount of Cu^{2+} is still not reduced to Cu_2O on the surface of electrode. It is shown from curves 3 and 4 of Fig. 4(b) that during the reverse scan, the photocurrent appears at 0.21 V, which is more positive than in the weakly alkaline solutions, as shown in curve 3 of Fig. 1(b) and in curve 2 of Fig. 3(b). CuO or $Cu(OH)_2$ has a larger solubility in a stronger alkaline solution (0.10 mol/L KOH), and hence a larger amount of CuO or $Cu(OH)_2$ dissolving in the solution,

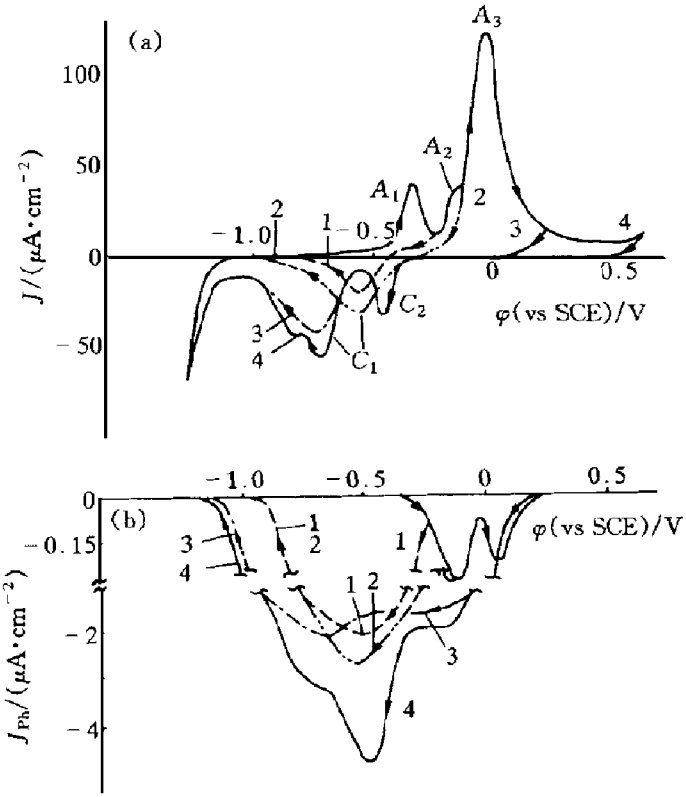

Fig. 4 (a) $J-\varphi$ curve and (b) $J_{ph}-\varphi$ curve for a Cu electrode in an argon-gas-purged 0.10 mol/L KOH solution at different anodic switching potentials φ_s

(Scan rate 2 mV·s^{-1}, modulation frequency 38 Hz, irradiation wavelength 420 nm)
1 —−0.24 V; 2 —−0.13 V; 3 —0.20 V; 4 —0.63 V

leaving a thin CuO or $Cu(OH)_2$ layer on the electrode surface. Therefore, on the reverse scan, the thin CuO or $Cu(OH)_2$ is easily reduced to Cu_2O, causing the photocurrent to appear at a more positive potential (+ 0.21 V), as shown in curves 3 and 4 of Fig. 4(b). In addition, a much larger photocurrent is observed on the reverse scan in 0.1 mol/L KOH solution, which suggests the presence of a more porous structure of the Cu_2O layer on the electrode surface[19].

Fig. 5(a) and Fig. 5(b) show, respectively, the $J-\varphi$ and $J_{ph}-\varphi$ plots for a Cu electrode in 0.05 mol/L Na_2SO_4 solution (pH 9.1) with and without argon-gas purging. In the case of argon-gas purging (curve 1), the passivating current plateau region cannot be observed on the $J-\varphi$ curve, and the cathodic photocurrent corresponding to the p-type response also cannot be measured, because the amount of Cu_2O on the electrode is very small. When the potential is close to the critical breakdown potential − 0.10 V on the positive scan, the anodic current (anodic dissolution of copper) greatly increases, and the anodic photocurrent appears at the same time. The corrosion products on the electrode, therefore, shows an n-type semiconducting property. In the non-deaerated solution (curve 2), an anodic current plateau in the potential region of − 0.26 to 0.04 V is observed when the potential becomes more positive than − 0.26 V. This current plateau is due to the formation of a Cu oxide layer, and the simultaneous electro-dissolution of Cu through the Cu oxide layer. It is shown in curve 2 of Fig. 5(b) that, on the positive potential scan, the cathodic photocurrent (the p-type response) increases with potential initially, and then decreases with increasing potential. The maximum cathodic photocurrent is at − 0.02 V. Hence, it is concluded that Cu_2O on the electrode appears around − 0.02 V. When the potential becomes more positive than 0.04 V, the critical breakdown potential of the passivated Cu, pitting corrosion occurs on the electrode surface[20], and the cathodic photocurrent gradually changes to the anodic photocurrent. The transition from the p- to the n-type photoresponse may be attributed to the doping of the surface Cu_2O film by the SO_4^{2-} ions[7].

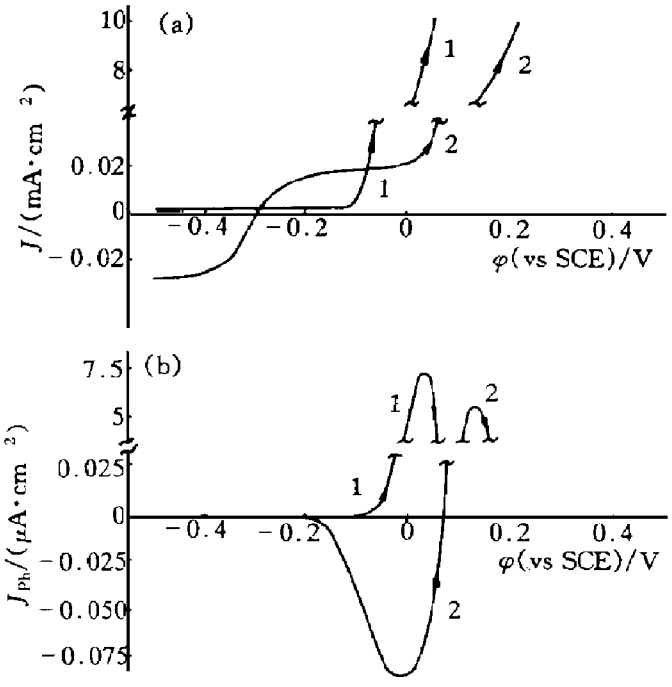

Fig. 5 (a) $J-\varphi$ curve and (b) $J_{ph}-\varphi$ curve for a Cu electrode in 0.05 mol/L Na_2SO_4 solution (pH 9.1)

(Scan rate 2 mV·s^{-1}, modulation frequency 38 Hz, irradiation wavelength 420 nm)

1—with argon-gas purging;

2—without argon-gas purging

4 CONCLUSIONS

The Cu electrode shows a p-type photoresponse in alkaline solutions, and changes to an n-type response in the alkaline Na_2SO_4 solution when the pitting corrosion occurs at potentials more positive than the critical breakdown potential. The cathodic photocurrent for the Cu electrode in non-deaerated solutions is smaller than in deaerated solutions, probably it is because oxygen enhances the anodic dissolution of copper, leaving a lesser amount of Cu_2O on the electrode surface. The appearance of CuO on the Cu electrode can be obtained from the $J_{ph}-\varphi$ curve. The potential of the initiation of CuO formation corresponds to the onset potential of the decrease in the cathodic photocurrent on the positive scan (or the potential at which the cathodic photocurrent is at its maximum). However, the initiation of CuO formation can hardly be seen from the $J-\varphi$ curve. The cathodic photocurrent

in strongly alkaline solution (e. g., 0. 1 mol/L KOH) is much larger than in weakly alkaline solution, suggesting the presence of a more porous structure of the Cu_2O layer on the electrode in the former case.

REFERENCES

1 Quarto F D, Piazza S and Sunseri C. Electrochim Acta, 1985, 30: 315.
2 Collisi U and Strehblow H H. J Electroanal Chem, 1986, 210: 213.
3 Collisi U and Strehblow H H. J Electroanal Chem, 1990, 284: 385.
4 Pan C Z, Yang M Z, Zhou G D and Cai S M. Acta Physico-Chimica Sinica, 1993, 9: 99.
5 Liu X Y, Zhou G D, Yang M Z, Cai S M and Loo B H. J Electroanal Chem, 1993, 361: 265.
6 Modestov A D, Zhou G D, Ge H H and Loo B H. J Electroanal Chem, 1994, 375: 293.
7 Modestov A D, Zhou G D, Ge H H and Loo B H. J Electroanal Chem, 1995, 380: 63.
8 Modestov A D, Zhou G D, Wu Y P, Notoya T and Schweinsberg D P. Corros Sci, 1994, 36: 1931.
9 Aruchamy A, Zhou G D and Fujishima A. J Electroanal Chem, 1988, 244: 333.
10 Zhou G D, Modestov A D, Pan C Z, Yang M Z and Cai S M. Acta Physico-Chimica Sinica, 1995, 11: 51.
11 Shao H, Zhou G D, Yang M Z and Cai S M. Acta Chimica Sinica, 1996, 54: 325.
12 Zhou G D, Shao H and Loo B H. J Electroanal Chem, 1997, 421: 129.
13 Trabanelli G, Zucchi F, Brunoro G and Bolognesi G P. Thin Solid Films, 1972, 13: 131.
14 Wilhelm S M, Tanizawa Y, Liu C Y and Hackerman N. Corros Sci, 1982, 22: 791.
15 Sutter E M M, Fiaud C and Lincot D. Electrochim Acta, 1993, 38: 1471.
16 Strehblow H H and Titze B. Electrochim Acta, 1980, 25: 839.
17 Stimming U. Electrochim Acta, 1986, 31: 415.
18 Castro A M, Medina L De, Marchiano S L and Arvia A J. J Appl Electrochem, 1978, 8: 121.
19 Kato C, Ateya B G, Castle J E and Pickering H W. J Electrochem Soc , 1980, 127: 1890.
20 Souto R M, Gonzalez S, Salvarezza R C and Arvia A J. Electrochim Acta, 1994, 38: 2619.

(Edited by Wu Jiaquan)